SUPPLEMENTARY MATERIAL

Phototransformation of the fungicide tebuconazole, and its predicted fate in sunlit surface freshwaters

Luca Carena, Andrea Scozzaro, Monica Romagnoli, Marco Pazzi, Luca Martone, Claudio Minero, Marco Minella, Davide Vione*

Dipartimento di Chimica, Università degli Studi di Torino, Via Pietro Giuria 5, 10125 Torino, Italy.

* Corresponding author. *davide.vione@unito.it*

Text S1. Chemicals and solvents

- Tebuconazole (TBCZ). $C_{16}H_{22}ClN_3O$; (RS)-1-(4-chlorophenil)-4,4-dimethyl-3-(1H,1,2,4-triazol-1-ylmethyl)pentan-3-ol; $\geq 98\%$; CAS: 107534-96-3; 307.82 g mol^{-1}; supplier: Sigma-Aldrich or TCI Chemicals.

- Hydrogen peroxide. H_2O_2; 30% (w/w) in H_2O; CAS: 7722-84-1; 34.01 g mol^{-1}; supplier: AppliChem Panreac.

- 2-Propanol. C_3H_8O; 100%; CAS: 67-63-0; 60.10 g mol^{-1}; supplier: VWR Chemicals BDH.

- Sodium nitrate. $NaNO_3$; $\geq 99\%$; CAS: 7631-99-4; 84.99 g mol^{-1}; supplier: Merck KGaA.

- Sodium bicarbonate. $NaHCO_3$; $\geq 99.7\%$; CAS: 144-55-8; 84.01 g mol^{-1}; supplier: Sigma-Aldrich.

- Sodium dihydrogen phosphate, monohydrate. $NaH_2PO_4 \times H_2O$; $\geq 99\%$; CAS: 10049-21-5; 137.99 gmol^{-1}; supplier: Sigma-Aldrich.

- 4-Carboxybenzophenone (CBBP). 99%; CAS: 611-95-0; 226.23 g mol^{-1}; supplier: Sigma-Aldrich.

- Phenol (PhOH). 99%; CAS: 108-95-2; 94.11 g mol^{-1}; supplier: Sigma-Aldrich.

- Rose Bengal (RB). 82.6%; CAS: 632-69-9; 1017.64 g mol^{-1}; supplier: Alfa Aesar.

- Furfuryl alcohol (FFA). 98%; CAS: 98-00-0; 98.10 g mol^{-1}; supplier: Sigma-Aldrich.

- 2-Nitrobenzaldehyde (2-NBA). 98%; CAS: 552-89-6; 151.12 g mol^{-1}; supplier: Sigma-Aldrich.

- Phosphoric acid. H_3PO_4; 85%; CAS: 7664-38-2; 97.99 g mol^{-1}; supplier: AppliChem Panreac.

- Sodium hydroxide. NaOH; 98%; CAS: 1310-73-2; 40.00 g mol^{-1}; supplier: Alfa Aesar.

- Methanol (MeOH). HPLC gradient grade; CAS: 67-56-1; 34.04 g mol^{-1}; supplier: VWR Chemicals BDH or Carlo Erba Reagents.

- Acetonitrile. CH_3CN; HPLC gradient grade; CAS: 75-05-8; 41.05 g mol^{-1}; supplier: VWR Chemicals BDH.

- Formic acid. HCOOH; 99.4%; CAS: 64-18-6; 46.03 g mol^{-1}; supplier: VWR Chemicals BDH.

Table S1 Collision energies applied to each experiment. TBCZ = tebuconazole.

Starting molecule	Ion (m/z)	Type of experiment	Collision Energy (eV)
TBCZ	308	MS^2	35
TBCZ	165	MS^3	25
TBCZ + $^\bullet$OH	324	MS^2	35
TBCZ + $^\bullet$OH	306	MS^3	25
TBCZ + $^\bullet$OH	322	MS^2	35
TBCZ + $^\bullet$OH	304	MS^3	25
TBCZ + $^\bullet$OH	224	MS^2	25
TBCZ + $^\bullet$OH	206	MS^3	25
TBCZ + $^\bullet$OH	272	MS^2	25
TBCZ + $^\bullet$OH	236	MS^3	25
TBCZ + ^{3}CBBP*	324	MS^2	35

Table S2. Photochemical reaction parameters of tebuconazole (TBCZ): direct photolysis quantum yield (Φ), and second-order reaction rate constants ($k_{PPRI,TBCZ}$) with the PPRIs $^\bullet$OH and ^{3}CDOM*. The reactions with $^1O_2$ and $CO_3^{\bullet-}$ can be neglected.

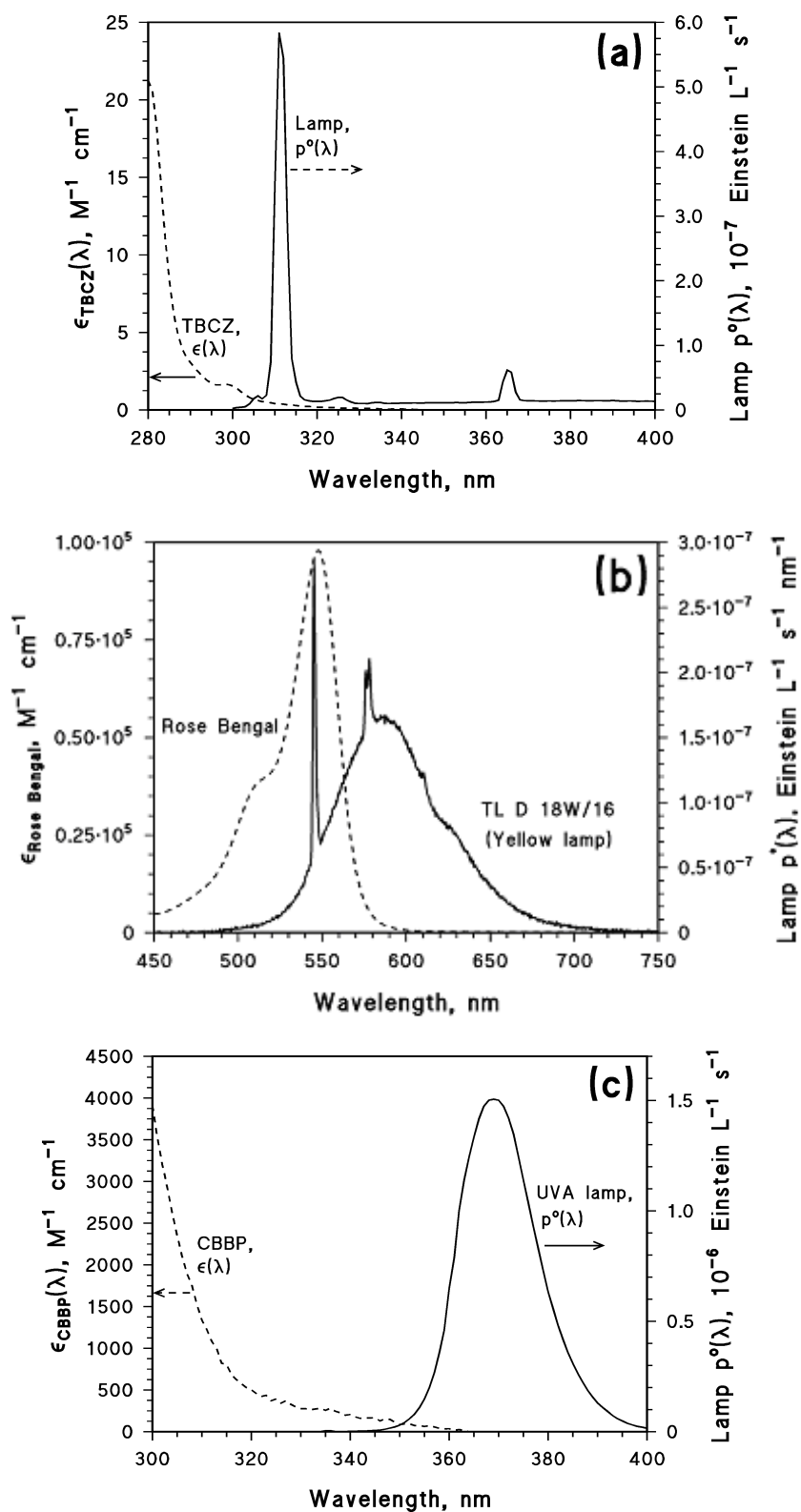|	TBCZ
Φ, unitless	0.22 ± 0.03
$k_{^\bullet OH,TBCZ}$, $\mathbf{M^{-1}\ s^{-1}}$	$(1.2\pm0.3) \times 10^{10}$
$k_{^3CDOM*,TBCZ}$, $\mathbf{M^{-1}\ s^{-1}}$	$(2.45\pm0.10) \times 10^8$

Figure S1. Absorption (molar absorption coefficients, $\varepsilon(\lambda)$) and emission spectra (spectral photon flux densities, $p°(\lambda)$) of: **(a)** TBCZ and UVB lamp; **(b)** Rose Bengal and yellow lamp; **(c)** CBBP and UVA lamp.
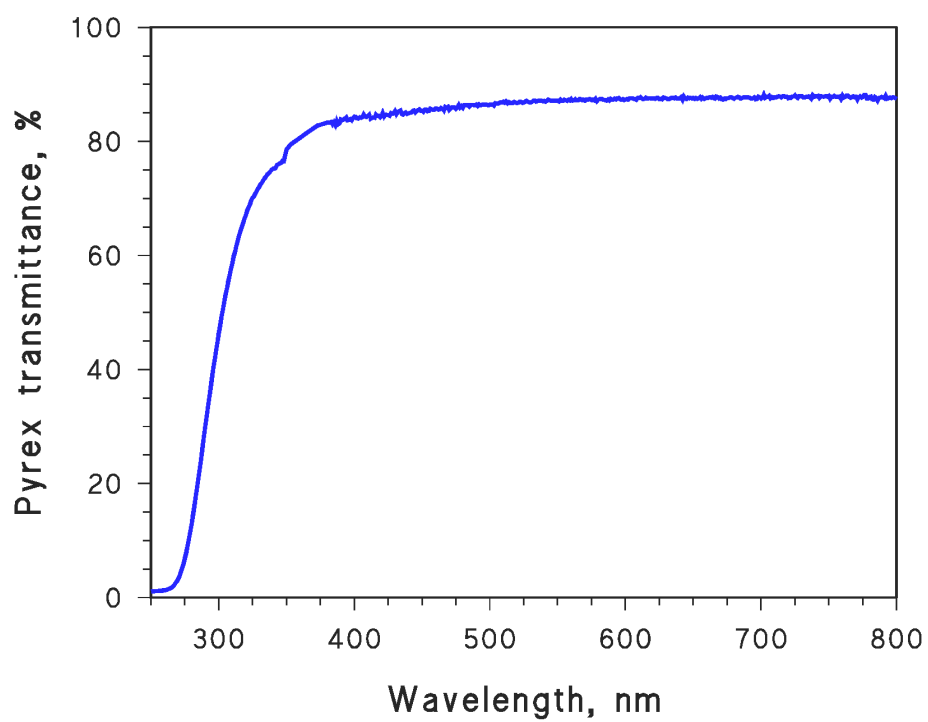
Figure S2. Transmittance spectrum of the Pyrex wall of the irradiation cells. The T% value at 300 nm is above 50%, the cut-off wavelength is around 280 nm.

Text S2. Reaction with $^1O_2$

Degradation of TBCZ by $^1O_2$ was assessed by irradiation of aqueous solutions at pH ~ 7, containing TBCZ (7, 14, or 20 µM) and Rose Bengal (RB, 10 µM), under a yellow lamp (**Figure S1b**). The possible reactions taking place in our irradiated solutions are reported below (**reactions S1-S3**). Limited photodegradation (< 15%) of the fungicide was observed after 24 h of irradiation, without any significant temporal trend of its concentration (**Figure S3**). This result suggests that singlet oxygen has a very low reactivity towards TBCZ, in agreement with results obtained with many other pollutants. Therefore, the value of k_2 would be negligible, when compared with the bimolecular rate constants of the TBCZ reactions with $^\bullet OH$ and $^3CDOM*$.

$$RB + h\nu + O_2 \rightarrow RB + {}^1O_2 \tag{S1}$$

$$TBCZ + {}^1O_2 \rightarrow Products \qquad [k_2] \tag{S2}$$

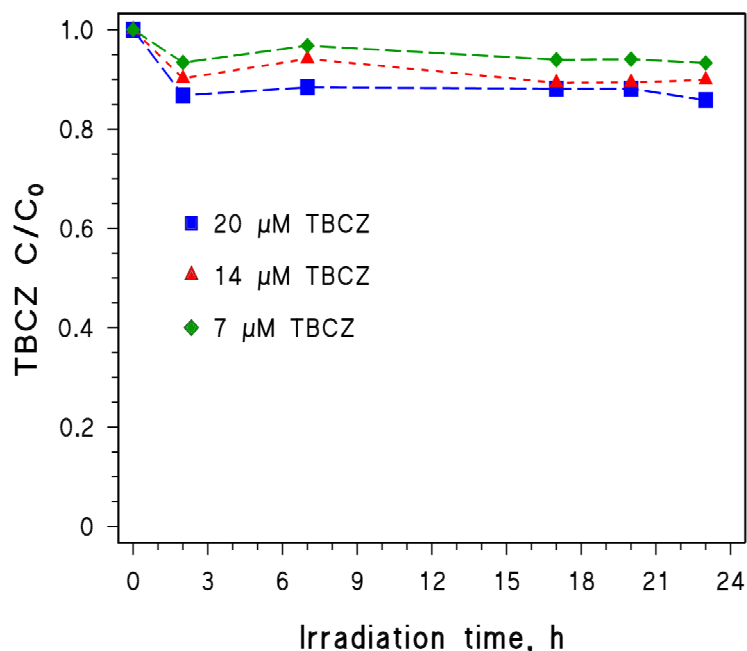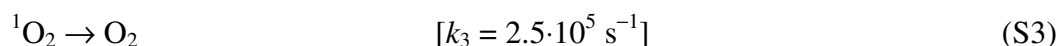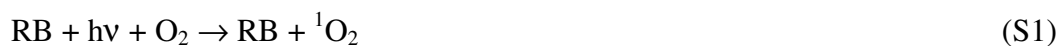$$^1O_2 \rightarrow O_2 \qquad [k_3 = 2.5 \cdot 10^5 \text{ s}^{-1}] \tag{S3}$$

Figure S3. Time trend of TBCZ upon irradiation with 10 µM RB, under the yellow lamp (reaction with $^1O_2$).

Supporting this finding, we measured the formation rate of $^1O_2$ ($R_{^1O_2}$) in our irradiated solutions, by exploiting the reactivity of $^1O_2$ with furfuryl alcohol (FFA). We irradiated 10 µM RB + 0.1 mM FFA, and monitored the transformation of FFA, which reacts with $^1O_2$ with rate constant k_{FFA} = $1.2 \cdot 10^8$ M^{-1} s^{-1} (Wilkinson and Brummer, 1981). The time evolution of FFA is shown in **Figure S4**, from which it was possible to obtain R_{FFA} = $(6.03 \pm 0.09) \cdot 10^{-8}$ M s^{-1} as the initial transformation rate of FFA (average of duplicate experiments). In the system containing RB + FFA, irradiated RB yields $^1O_2$ (**reaction S1**) that can either undergo thermal deactivation (**reaction S3**), or react with FFA. Upon application of the steady-state approximation to $^1O_2$, one obtains the following equation for $R_{^1O_2}$:

$$R_{^1O_2} = R_{FFA} \cdot \frac{k_3 + k_{FFA} \cdot C_{FFA}}{k_{FFA} \cdot C_{FFA}} \tag{S4}$$

where C_{FFA} = $1 \cdot 10^{-4}$ M. From **Eq. (S4)** one gets $R_{^1O_2}$ = $(1.32 \pm 0.02) \cdot 10^{-6}$ M s^{-1}. Therefore, singlet oxygen was actually produced in our irradiated solutions, but it did not significantly react with TBCZ.

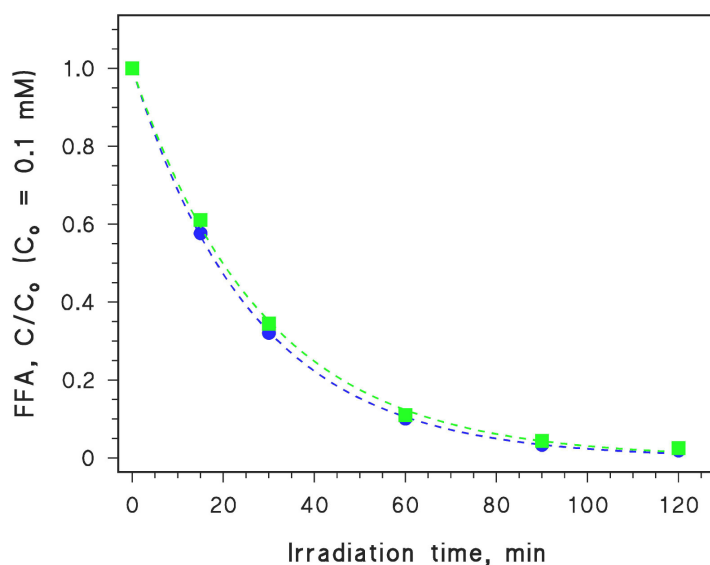**Figure S4.** Time trend of FFA (initial concentration 0.1 mM), upon irradiation of 10 µM RB under the used yellow lamp (Philips TL D Yellow) at pH 7. The results of duplicate experiments are shown here.
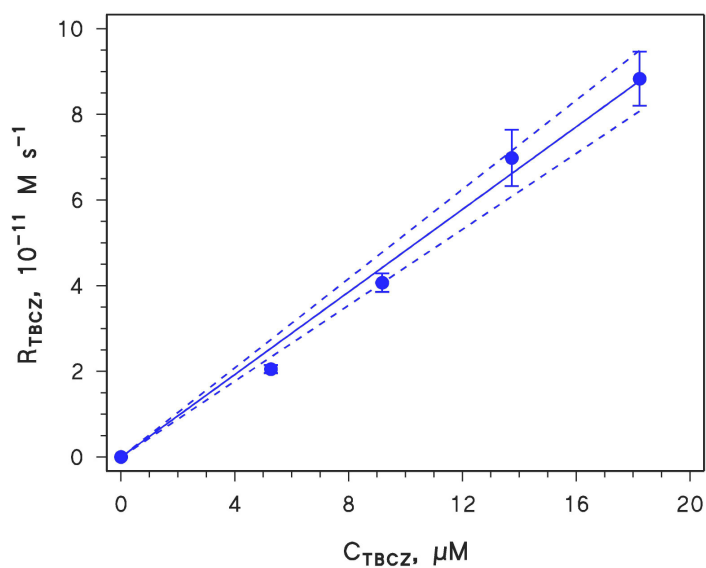
Figure S5. Initial TBCZ transformation rates (R_{TBCZ}), upon irradiation with 67 μM 4-carboxybenzophenone (CBBP) under the UVA lamp, as a function of the initial concentration of TBCZ (C_{TBCZ}). The solution pH was around 7. The fit line is solid, while the dashed lines represent the 95% confidence limits of the fit. The error bounds to the rate data represent ±σ.
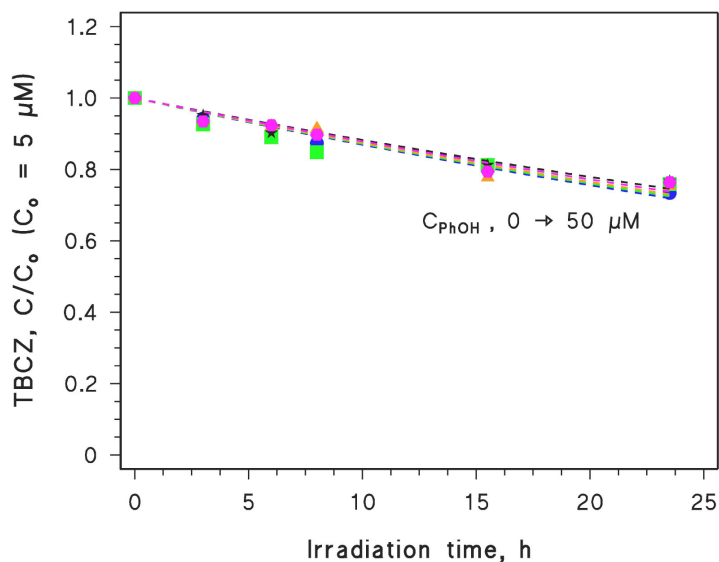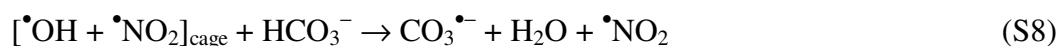

Figure S6. Time trend of TBCZ (initial concentration 5 μM), upon irradiation in the presence of 67 μM 4-carboxybenzophenone (CBBP) under the UVA lamp, for different values of phenol added in the concentration range of 0-50 μM. The solution pH was around 7.

Text S3. Reaction with $CO_3^{\bullet-}$

To assess the reactivity between TBCZ and $CO_3^{\bullet-}$, we used here a semi-quantitative screening method that makes use of nitrate and bicarbonate under UVB irradiation (Vione et al., 2009). The rationale of the method is that nitrate photolysis yields $^\bullet OH$ and $^\bullet NO_2$ as photogenerated fragments, inside a cage of water molecules ($[^\bullet OH + {}^\bullet NO_2]_{cage}$). The geminate species inside the cage can either recombine back to nitrate, or diffuse into the solution bulk. Once in the bulk, $^\bullet OH$ can react with dissolved substrates like TBCZ (Mark et al., 1996; Bouillon and Miller, 2005). The ions HCO_3^- and CO_3^{2-} can react with both bulk and cage $^\bullet OH$ to yield $CO_3^{\bullet-}$, which is considerably less reactive than the hydroxyl radical. However, the reaction of HCO_3^- / CO_3^{2-} with cage $^\bullet OH$ would inhibit photofragment recombination to nitrate (reactions S5-S11).

$$NO_3^- + h\nu + H^+ \rightarrow [^\bullet OH + {}^\bullet NO_2]_{cage} \qquad (S5)$$

$$[^\bullet OH + {}^\bullet NO_2]_{cage} \rightarrow {}^\bullet OH + {}^\bullet NO_2 \qquad (S6)$$

$$[^\bullet OH + {}^\bullet NO_2]_{cage} \rightarrow NO_3^- + H^+ \qquad (S7)$$

$$[^\bullet OH + {}^\bullet NO_2]_{cage} + HCO_3^- \rightarrow CO_3^{\bullet-} + H_2O + {}^\bullet NO_2 \qquad (S8)$$

$$[^\bullet OH + {}^\bullet NO_2]_{cage} + CO_3^{2-} \rightarrow CO_3^{\bullet-} + OH^- + {}^\bullet NO_2 \qquad (S9)$$

$$^\bullet OH + HCO_3^- \rightarrow CO_3^{\bullet-} + H_2O \qquad (S10)$$

$$^\bullet OH + CO_3^{2-} \rightarrow CO_3^{\bullet-} + OH^- \qquad (S11)$$

Because of the inhibition of photofragment ($[^\bullet OH + {}^\bullet NO_2]_{cage}$) recombination, the formation rate of $CO_3^{\bullet-}$ in the presence of nitrate + bicarbonate would be significantly higher than the formation rate of $^\bullet OH$ with nitrate alone (Bouillon and Miller, 2005). Because HCO_3^- and CO_3^{2-} induce the formation of a higher amount of a less reactive species, one expects different effects depending on the reactivity of a dissolved substrate with $CO_3^{\bullet-}$ *vs.* $^\bullet OH$. If the substrate is poorly reactive toward $CO_3^{\bullet-}$, its photodegradation would be inhibited by bicarbonate. In contrast, the degradation of substrates that are reactive enough with $CO_3^{\bullet-}$ would be enhanced by bicarbonate (Vione et al., 2009). However, the addition of bicarbonate to nitrate also modifies the solution pH, which may possibly modify acid-base equilibria, with potential impacts on nitrate photolysis and substrate reactivity. Therefore, the effect of bicarbonate is compared to the degradation of the substrate, with nitrate and a phosphate buffer ($NaH_2PO_4 + Na_2HPO_4$), at the same concentration (comparable ionic strength) and pH of $NaHCO_3$.

Figure S7 reports the initial transformation rates of 20 µM TBCZ, upon UVB irradiation in the presence of: *(i)* 10 mM $NaNO_3$ and variable $NaHCO_3$ concentrations; *(ii)* variable $NaHCO_3$

concentrations; *(iii)* 10 mM NaNO$_3$ and a phosphate buffer, at the same concentration of NaHCO$_3$ and same pH (within ±0.1 units).

The experimental data show that the addition of bicarbonate inhibits the photodegradation of TBCZ in the presence of nitrate, while the direct photolysis of TBCZ is negligible under all conditions. These results suggest that TBCZ does not undergo important reaction with CO$_3^{\bullet-}$, which can thus be neglected as far as the photochemical fate of TBCZ is concerned.
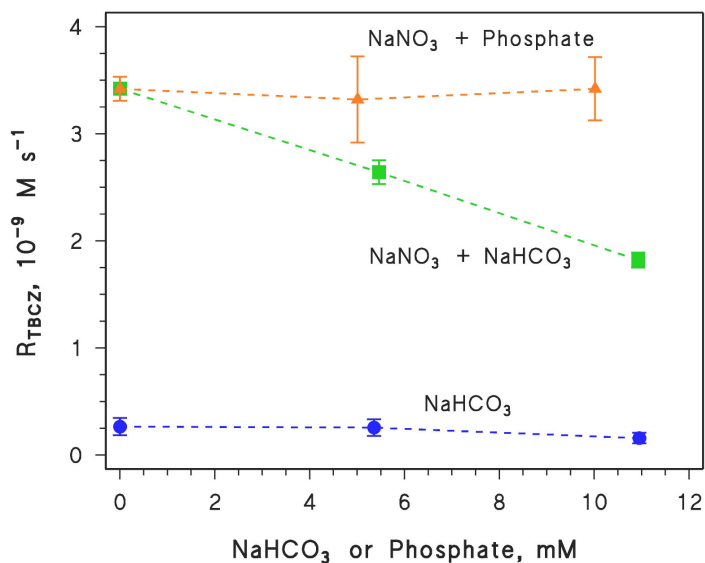

Figure S7. Initial transformation rates under UVB irradiation of (■) 20 μM TBCZ and 10 mM NaNO$_3$, as a function of the concentration of NaHCO$_3$; (▲) 20 μM TBCZ and 10 mM NaNO$_3$, as a function of the concentration of added phosphate buffer (same concentration as NaHCO$_3$ and same pH, within 0.1 units); (◆) 20 μM TBCZ, without nitrate, as a function of NaHCO$_3$ concentration.
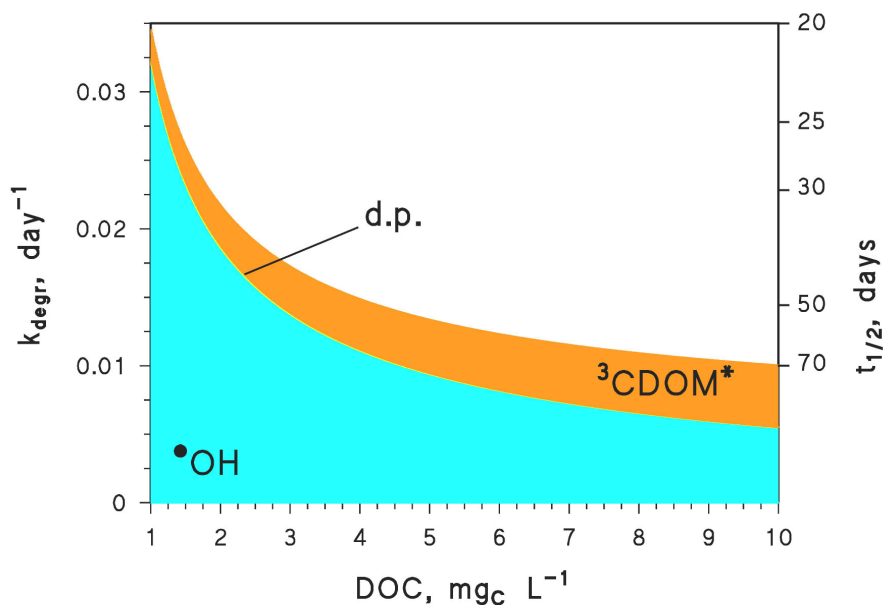
Figure S8. Modelled first-order photodegradation rate constants of TBCZ (left Y-axis), together with the corresponding half-life times (right Y-axis) ($t_{1/2} = \ln 2 \; k_{degr}^{-1}$), as a function of varying dissolved organic carbon (DOC). Assumed water conditions: depth $d = 5$ m, $[NO_3^-] = 10^{-4}$ M, $[NO_2^-] = 10^{-6}$ M, $[HCO_3^-] = 10^{-3}$ M, $[CO_3^{2-}] = 10^{-5}$ M. Days correspond to fair-weather 15 July at 45°N latitude. Calculations were carried out with the APEX software; the coloured areas of the graph highlight the importance of the different photodegradation pathways (d.p. = direct photolysis).
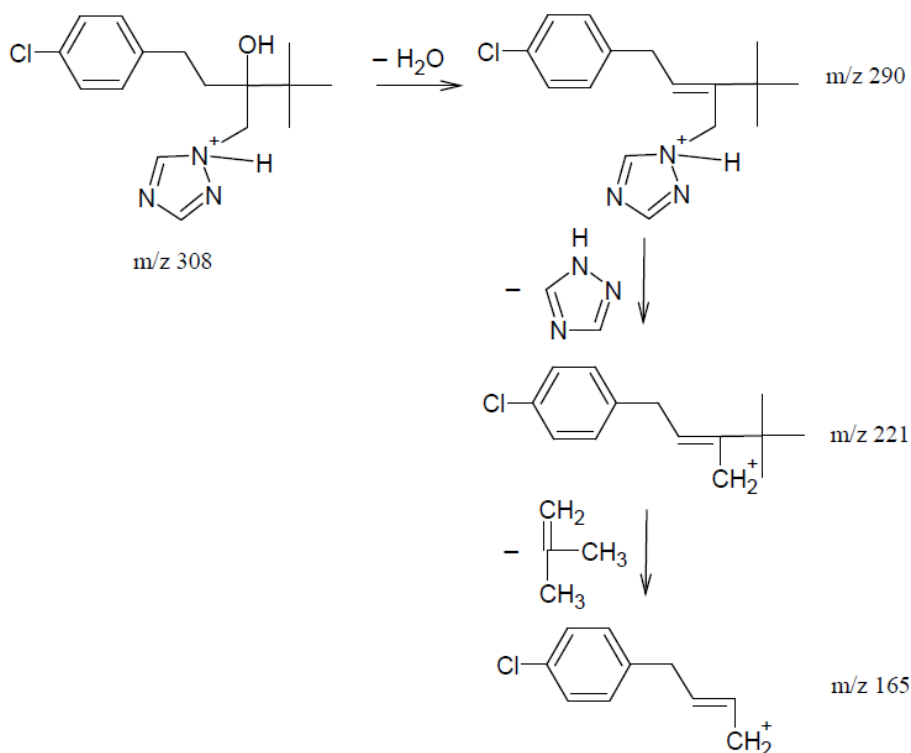
Figure S9 Fragmentation pathway of tebuconazole ([M + H]$^+$ 308). Adapted from Calza et al. (2002).

Text S4. Identification of the intermediates formed upon TBCZ reaction with $^\bullet$OH.

This section describes the identification of the photoproducts of TBCZ oxidation by $^\bullet$OH. Identification was possible thanks to comparison with literature findings, concerning the heterogeneous photocatalytic (TiO$_2$ + hν) degradation of TBCZ reported by Calza et al. (2002). The photocatalytic process forms reactive species, with similar reactivity to free $^\bullet$OH in solution. In the following paragraphs, we describe the results obtained by LC-MS^n analysis of the sample TBCZ + H$_2$O$_2$ + UVB.

Three ions at m/z 324 were found, which could be the hydroxylated products of TBCZ, produced by $^\bullet$OH radical attack. The radical $^\bullet$OH can attack different portions of the TBCZ molecule (Calza et al., 2002), which would explain the presence of different intermediates with the same mass-charge ratio (see **Figure S10**). There were some common losses between TBCZ and its hydroxylated products, for which the loss of two water molecules was observed to produce the ions with m/z 306

and 288. This finding confirms the presence of a second alcoholic group, compared to the initial TBCZ.

A MS^3 experiments was carried out, by focusing on the ion with m/z 306. Here it was possible to notice the loss of a second water molecule from the first and third species (t_R = 16.00 min and t_R = 19.66 min), which enabled the assumption that hydroxylation occurred in a position favourable to water loss (e.g., the methylene groups on the aliphatic chain). The ion with m/z 237 was produced by loss of the triazole part, while the m/z 181 ion resulted from the loss of a lateral aliphatic chain (see **Figure S11**). In the second species (t_R = 18.86 min), the loss of a second water molecule was not observed. However, the presence of ions at m/z 237 and 181 suggests that hydroxylation did not occur on the triazole or the butyl group. Moreover, the absence of an ion with m/z 288 allows for oxidation of the methylene chain to be ruled out. Therefore, it could be assumed that hydroxylation occurred on the chlorobenzyl group, and possibly in ortho position when considering the presence and the likely effect of chlorine on the ring (see **Figure S12**). The hypothesised structures of these intermediates are shown in **Table 2** of the main manuscript.

The ion at m/z 322 could result from oxidation of the alcoholic group in the hydroxylated molecule, leading to the formation of a ketone. The MS^2 experiment carried out from m/z 322 showed loss of a water molecule, to produce m/z 304. The m/z 304 ion was subject in turn to a MS^3 experiment, which highlighted losses of triazole and butyl (producing the fragments at m/z 235 and 179, respectively). As proposed by Calza et al. (2002), the initial loss of water would be an evidence that hydroxylation (taking place before oxidation of the alcoholic group to the ketone) occurred on the methylene group near the aromatic ring. In contrast, no water loss would be expected if hydroxylation occurred in a vicinal position to the TBCZ alcoholic group (see **Figure S13**) (Calza et al., 2002).

Another photodegradation pathway could be studied by MS^2 analysis of the ion at m/z 224 (see **Figure S14**), followed by MS^3 analysis of the ion at m/z 206. The loss of CO from m/z 206 could be noted, through the occurrence of the ion at m/z 178.

The ion at m/z 272 could originate by double hydroxylation of the aromatic ring, and fragmentation could produce m/z 236 by loss of two water molecules. The MS^3 analysis, performed on m/z 236, showed loss of triazole followed by butyl, or vice versa (see **Figure S15**) (Calza et al., 2002).
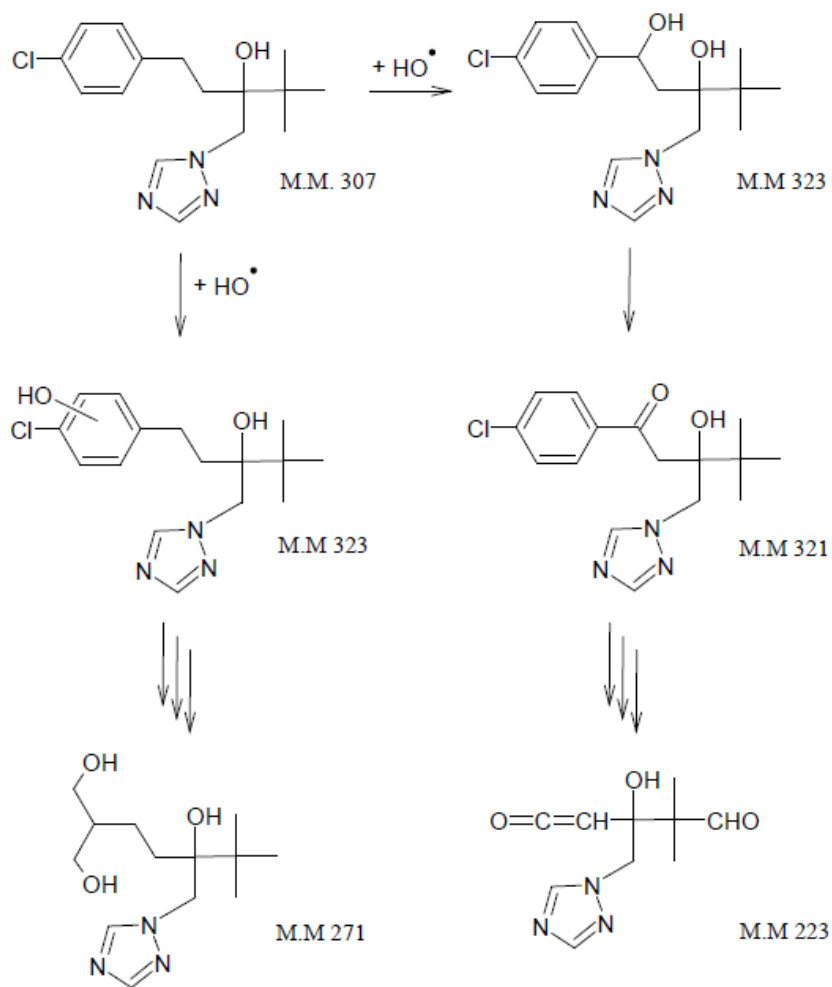
Figure S10. Fragmentation pathways following oxidation by hydroxyl radicals. Adapted from Calza et al. (2002).
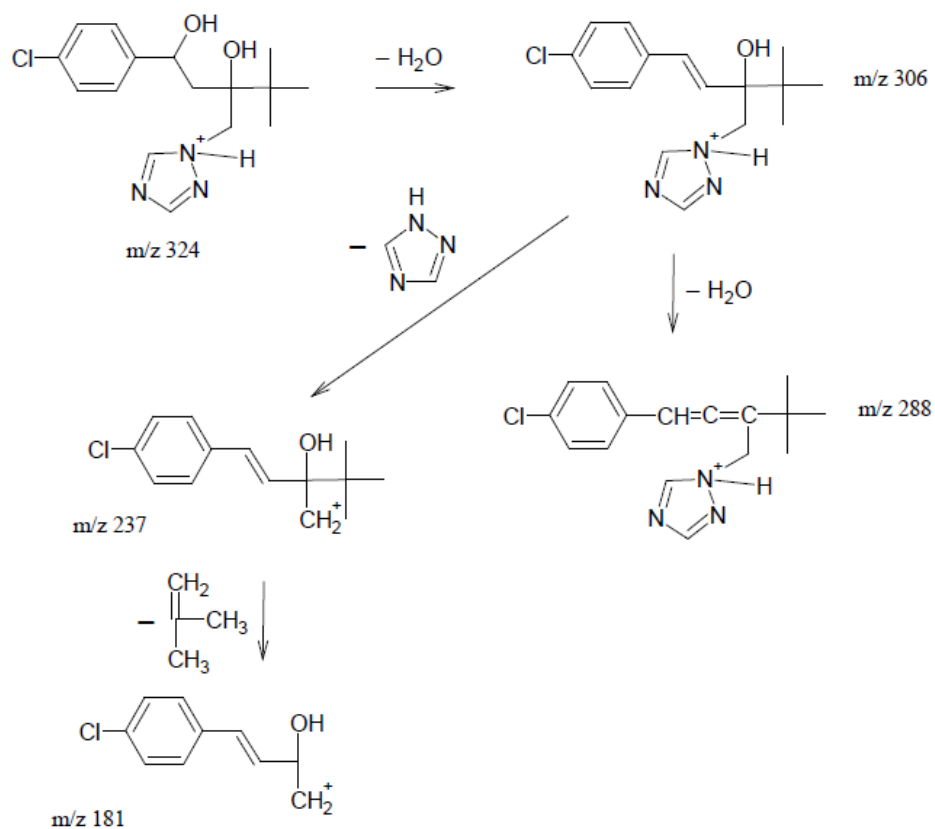
Figure S11. Fragmentation pathway of the species having $[M + H]^+$ 324. Adapted from Calza et al. (2002).
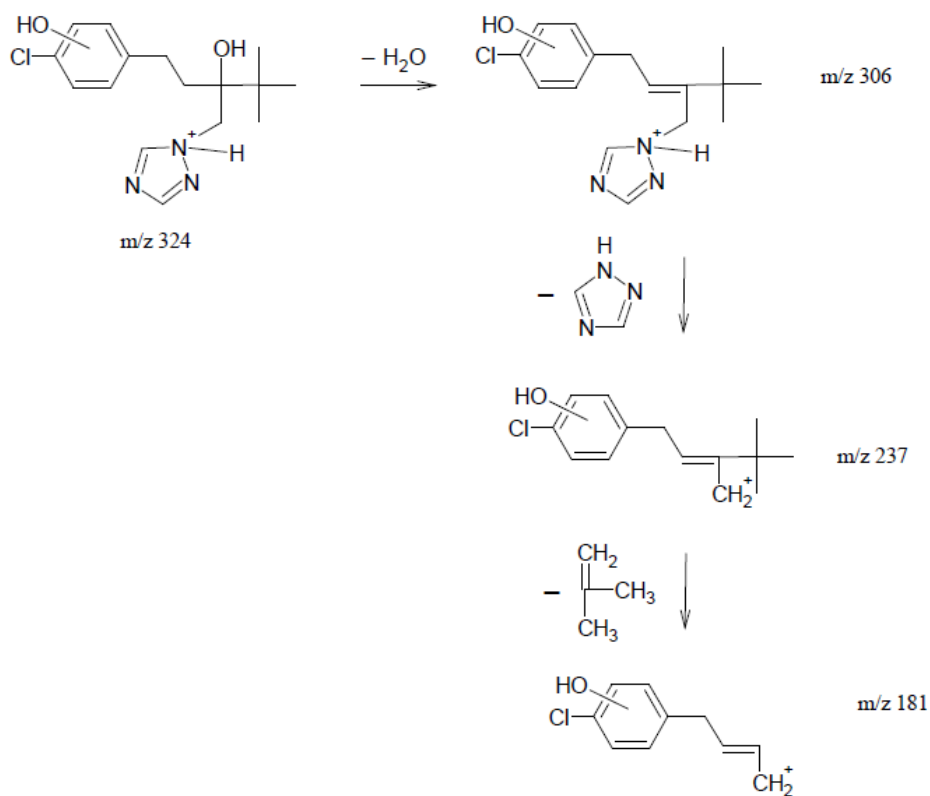

Figure S12. Fragmentation pathway of another species having $[M + H]^+$ 324. Adapted from Calza et al. (2002).
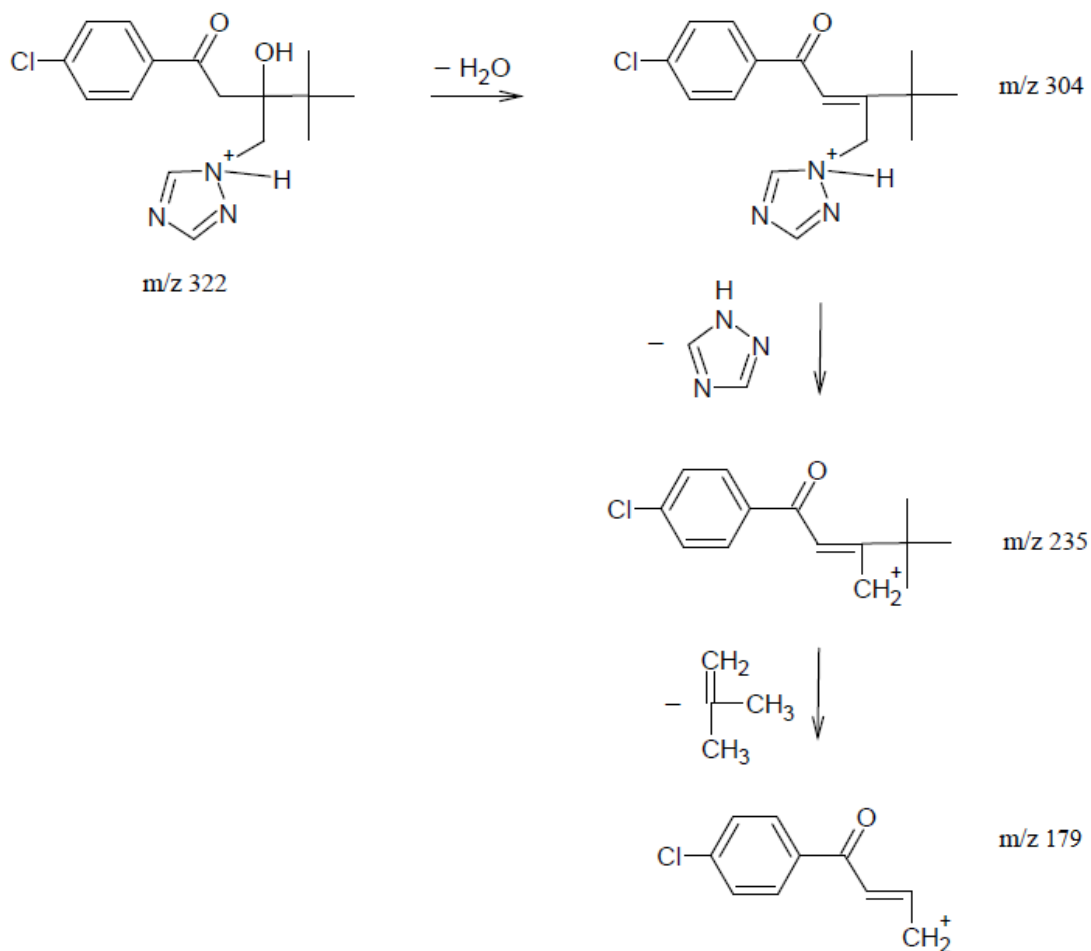
Figure S13. Fragmentation pathway of the species having [M + H]$^+$ 322. Adapted from Calza et al. (2002).
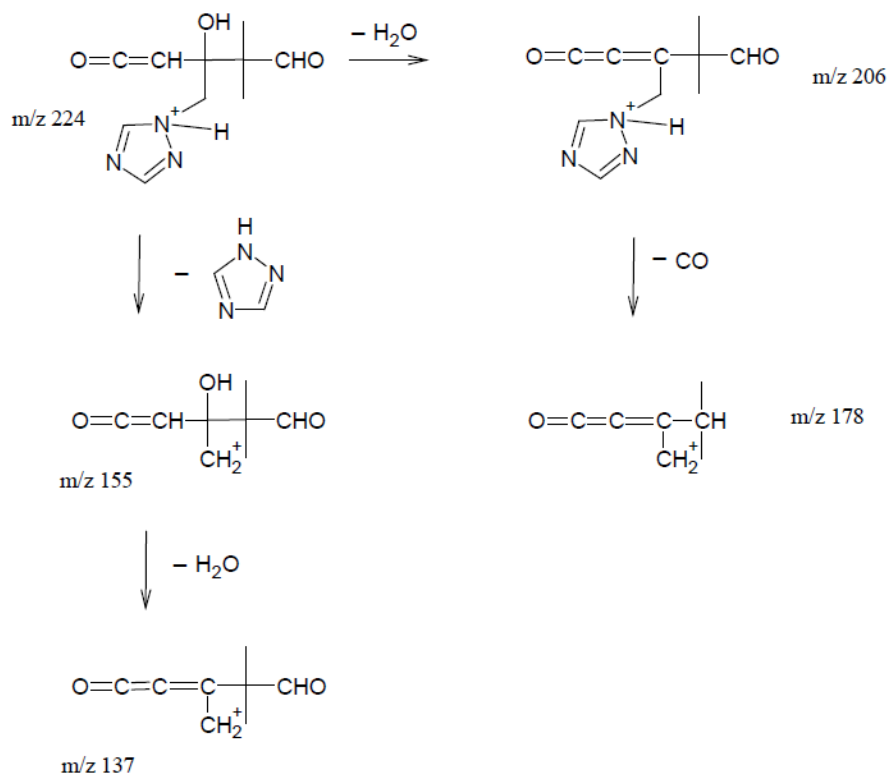
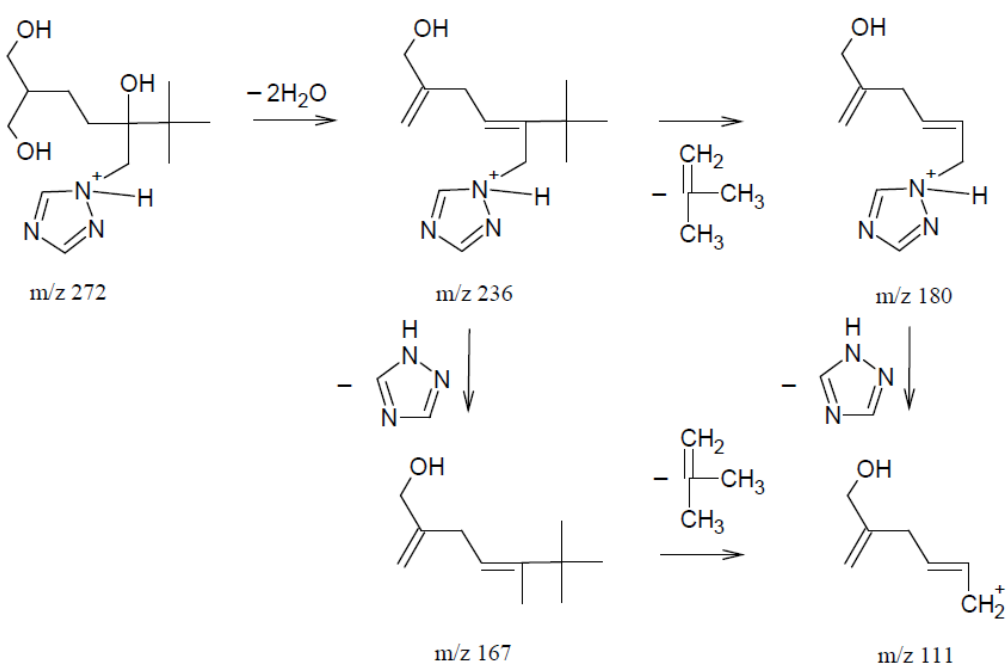**Figure S14.** Fragmentation pathway of the species having $[M + H]^+$ 224. Adapted from Calza et al. (2002).

Figure S15. Fragmentation pathway of the species having $[M + H]^+$ 272. Adapted from Calza et al. (2002).

References

Bouillon, R. C., Miller, W. L., 2005. Photodegradation of dimethyl sulfide (DMS) in natural waters: Laboratory assessment of the nitrate-photolysis-induced DMS oxidation. Environ. Sci. Technol. 39, 9471-9477.

Calza, P., Baudino, S., Aigotti, R., Baiocchi, C., Branca, P., Pelizzetti, E., 2002. High-performance liquid chromatographic/tandem mass spectrometric identification of the phototransformation products of tebuconazole on titanium dioxide. J. Mass Spectrom. 37, 566-576.

Mark, G., Korth, H. G., Schuchmann, H. P., von Sonntag, C., 1996. The photochemistry of aqueous nitrate ion revisited. J. Photochem. Photobiol. A: Chem. 101, 89-103.

Vione, D., Khanra, S., Cucu Man, S., Maddigapu, P. R., Das, R., Arsene, C., Olariu, R. I., Maurino, V., Minero, C., 2009. Inhibition vs. enhancement of the nitrate-induced phototransformation of organic substrates by the $^\bullet$OH scavengers bicarbonate and carbonate. Water Res. 43, 4718-4728.

Wilkinson, F., Brummer, J., 1981. Rate constants for the decay and reactions of the lowest electronically excited singlet-state of molecular oxygen in solution. J. Phys. Chem. Ref. Data 10, 809-1000.